



# International Journal of Medical and All Body Health Research

## Development of a Label-Free Electrochemical Biosensor for Early Detection of Neurodegenerative Disease Biomarkers

Ibukunoluwa Fikayo Olukotun <sup>1\*</sup>, Akuchinyere Onyinyechukwu Titus-Okpanachi <sup>2</sup>, Rachael Taiwo Tiamiyu <sup>3</sup>, Ehinomhen Inegbedion <sup>4</sup>

<sup>1</sup> Department of Analytical Bioscience, Birkbeck University of London, London, United Kingdom

<sup>2</sup> Department of Public and Community Health, Liberty University, Virginia, USA

<sup>3</sup> Department: Department of Chemistry, Wayne State University, Michigan, USA

<sup>4</sup> Department of Healthcare Management, Western Governors University, Salt Lake City, Utah, USA

\* Corresponding Author: **Ibukunoluwa Fikayo Olukotun**

### Article Info

ISSN (online): 2582-8940

Volume: 06

Issue: 02

April-June 2025

Received: 03-02-2025

Accepted: 05-03-2025

Page No: 61-66

### Abstract

Early diagnosis of neurodegenerative diseases (NDs) such as Alzheimer's (AD) and Parkinson's (PD) is critically dependent on detecting specific protein biomarkers at very low concentrations. This study presents the design, fabrication, and characterization of a novel label-free electrochemical biosensor for ultrasensitive detection of key ND biomarkers ( $\beta$ -amyloid ( $A\beta$ ), tau, and  $\alpha$ -synuclein). A glassy carbon electrode (GCE) was modified with a nanocomposite of carboxyl graphene (CG), thionin, and electrodeposited Au nanoparticles (AuNPs) to immobilize a specific aptamer against tau protein. Electrochemical techniques (cyclic voltammetry (CV) and electrochemical impedance spectroscopy (EIS)) were used to verify each modification step, and differential pulse voltammetry (DPV) was used to measure biomarker binding. The sensor yielded a linear response from 0.5 pM to 100 pM tau<sub>381</sub>, with a detection limit (LOD) of ~0.5 pM and high sensitivity. These performance metrics are comparable to or exceed those of previously reported label-free biosensors. Cross-reactivity tests showed excellent selectivity against non-target proteins. The fabricated biosensor demonstrates rapid, reproducible detection of tau at clinically relevant levels, addressing key research questions: (1) *Can a label-free electrochemical biosensor be engineered to detect neurodegenerative biomarkers at ultra-low concentrations?* (2) *What sensitivity and specificity can be achieved through nanomaterial-enhanced signal transduction?* (3) *How does this sensor performance compare with existing biosensing platforms?* In answering these questions, this work contributes to the development of point-of-care ND diagnostics.

DOI: <https://doi.org/10.54660/IJMBHR.2025.6.2.61-66>

**Keywords:** Label-free electrochemical biosensor, Neurodegenerative disease biomarkers, Tau protein detection, Nanomaterial-enhanced sensing, Differential pulse voltammetry (DPV), Point-of-care diagnostics

### 1. Introduction

Neurodegenerative diseases (NDs) such as Alzheimer's disease (AD) and Parkinson's disease (PD) are increasing global health challenges due to aging populations. AD is characterized by extracellular  $\beta$ -amyloid ( $A\beta$ ) plaques and intracellular hyperphosphorylated tau tangles in the brain, while PD involves accumulation of  $\alpha$ -synuclein into Lewy bodies. The concentrations of these biomarkers in accessible biofluids (blood, cerebrospinal fluid) are extremely low, often in the picomolar (pM) or even femtomolar range. Conventional diagnostic methods (e.g. MRI/PET imaging, ELISA of cerebrospinal fluid) are invasive, costly, or lack the sensitivity for early-stage detection. Electrochemical biosensors offer a promising alternative: by

exploiting nanomaterial-modified electrodes and specific biorecognition elements (antibodies or aptamers), they can achieve high sensitivity and rapid response in a label-free format.

These devices are inherently amenable to miniaturization and point-of-care use, potentially enabling early ND diagnosis.

In the context of AD and PD, key protein biomarkers include A $\beta$ <sub>40/42</sub> and tau (AD), and  $\alpha$ -synuclein (PD). Table 1 (see below) summarizes their relevance. Prior work has demonstrated electrochemical sensors for each biomarker, often using redox-active probes or labels. However, label-free detection (e.g. via impedance or direct voltammetric signal) simplifies the assay and can improve sensitivity and speed. For example, Rushworth *et al.* reported a label-free impedimetric sensor using a prion protein fragment to bind A $\beta$  oligomers, achieving detection down to ~0.5 pM. Similarly, recent immunosensors and aptasensors have reached sub-pM LODs for these targets. Nevertheless, there remains a need to optimize sensor design (electrode materials, surface chemistry) for even greater performance and practical usability.

This study addresses the following research questions:

1. Can a label-free electrochemical biosensor be designed and fabricated to detect neurodegenerative biomarkers (A $\beta$ , tau,  $\alpha$ -synuclein) at clinically relevant (pM) concentrations?
2. What is the sensitivity (LOD, linear range, signal-to-noise) achieved by a nanomaterial-enhanced sensor using impedance/voltammogram readouts?

3. How does the new sensor's performance compare quantitatively with existing label-free biosensors reported in the literature?

To answer these questions, we performed a thorough literature review of AD/PD biomarkers and prior electrochemical sensors (Section 3), then developed an experimental methodology for sensor fabrication and electrochemical characterization (Section 4). Results (Section 5) include historical performance data and in-depth analysis of our findings. The work concludes with insights on how the proposed sensor advances early ND diagnosis, fulfilling the stated objectives.

## Literature Review

### Neurodegenerative Biomarkers (A $\beta$ , Tau, $\alpha$ -Synuclein)

Alzheimer's disease is widely studied for its hallmark biomarkers: A $\beta$  peptides (particularly A $\beta$ <sub>42</sub>) and tau protein variants. A $\beta$  originates from amyloid precursor protein cleavage, aggregating into plaques that are neurotoxic. Total tau (t-tau) and phosphorylated tau (p-tau) become elevated in AD due to neurofibrillary tangles. Similarly, Parkinson's disease is associated with accumulation of  $\alpha$ -synuclein ( $\alpha$ -syn) into Lewy bodies. These biomarkers can appear in blood or cerebrospinal fluid at very low levels: for example, AD patients have plasma tau on the order of a few pg/mL, while  $\alpha$ -syn in serum or CSF is typically low picomolar. Table 1 summarizes the known biomarkers, associated diseases, and typical concentration ranges.

**Table 1:** Key neurodegenerative disease biomarkers and their typical concentrations. AD = Alzheimer's disease; PD = Parkinson's disease; CSF = cerebrospinal fluid.

Biomarker	Associated Disease	Typical Biofluid Concentration	Clinical Significance
A $\beta$ <sub>42</sub> (amyloid-beta 42)	AD	CSF: ~500–1000 pg/mL (decreased in AD); Plasma: <<100 pg/mL	Key for amyloid pathology in AD
A $\beta$ <sub>40</sub> (amyloid-beta 40)	AD	CSF: ~1000–1500 pg/mL; Plasma: <<100 pg/mL	Ratio A $\beta$ <sub>42/40</sub> often used diagnostically
Total Tau (t-tau)	AD	CSF: ~200–300 pg/mL ( $\uparrow$ in AD); Plasma: ~1–5 pg/mL	Marker of neurodegeneration
Phospho-Tau (p-tau)	AD	CSF: ~20–60 pg/mL ( $\uparrow$ in AD)	Indicates Tau hyperphosphorylation
$\alpha$ -Synuclein	PD, Lewy body diseases	CSF: ~500–2000 pg/mL; Plasma: ~100–300 pg/mL	Primary component of Lewy bodies

Early changes in biomarker levels precede clinical symptoms by years, making them valuable for preclinical diagnosis. However, their low abundance demands ultrasensitive assays. Conventional laboratory assays (ELISA, immunoblotting, neuroimaging) often require invasive sampling or bulky equipment, and may not detect femtomolar concentrations. Therefore, there is great interest in developing minimally invasive point-of-care tests for these proteins, ideally using blood samples. Electrochemical biosensors have emerged as a promising strategy, due to their ability to transduce binding events into measurable electrical signals with high sensitivity.

### Electrochemical Label-Free Biosensors for ND Biomarkers

Electrochemical biosensors convert biorecognition events (antibody/aptamer binding) into electrical signals (current, voltage, impedance). In label-free formats, no secondary label (enzyme, nanoparticle) is needed; signal changes arise directly from surface events (e.g. impedance increase upon binding). This offers simplicity and real-time measurement. According to recent reviews, a variety of label-free electrochemical sensors have been reported for A $\beta$ , tau, and

$\alpha$ -syn. These sensors typically use modified electrodes to improve biocompatibility and signal strength. Common strategies include functionalizing with self-assembled monolayers (SAMs), nanomaterials (graphene, carbon nanotubes, metal nanoparticles), and conductive polymers. For example, Shiravandi *et al.* developed a label-free SAM/Au electrode immunosensor for cis p-tau with detection down to ~0.46 pg/mL ( $\approx$ 10 pM). Another recent device employed a hexagonal boron nitride (hBN) nanocomposite for tau, achieving LOD ~0.42 pg/mL ( $\approx$ 9.5 pM).

**Performance of published sensors:** Table 2 summarizes selected label-free electrochemical biosensors from the literature. For A $\beta$  detection, Rushworth *et al.* used an impedimetric sensor with a prion protein fragment, yielding linear response down to ~0.5 pM. Kaushik *et al.* reported a label-free immunosensor on a modified Au electrode, with LOD 10 pM for A $\beta$ (1–42). For tau detection, Tao *et al.* constructed an aptasensor (CG/thionin/AuNP on GCE) for tau<sub>381</sub>, with a linear DPV response from 1–100 pM and LOD 0.70 pM. For  $\alpha$ -synuclein, Ricci *et al.* demonstrated a polymer-organic transistor (EGOFET) sensor in microfluidics, achieving sub-pM detection range. Carneiro *et al.* developed a nanostructured immunosensor for  $\alpha$ -syn with

range 0.01–10 ng/mL ( $\approx 0.7$ –700 pM) and LOD  $\sim 4.1$  pg/mL ( $\sim 0.3$  pM).

**Table 2:** Examples of recent label-free electrochemical biosensors for neurodegenerative biomarkers. *Abbreviations:* Rct = charge-transfer resistance (impedance), DPV = differential pulse voltammetry, IDE = interdigitated electrode, EGOFET = electrolyte-gated organic field-effect transistor. Values of linear range (LR) and detection limit (LOD) are given in the units of analyte concentration. Data from cited references.

Biomarker (Target)	Sensor Type (Electrode)	Detection Method	Linear Range	LOD	Ref.
A $\beta$ oligomers	Au SPE + PrP fragment	EIS	–	$\sim 0.5$ pM	[20]
A $\beta_{1-42}$	Au IDE + SAM (DTSP)	DPV / EIS	10 pM – 100 nM	10 pM	[7]
Tau <sub>381</sub> (1N3R aptamer)	GCE + CG/TH/AuNP (aptamer)	DPV	1.0 pM – 100 pM	0.70 pM	[11]
$\alpha$ -Synuclein	Organic EGOFET (microfluidic)	FET/Amperometry	0.25 pM – 25 nM	sub-pM	[15]
$\alpha$ -Synuclein	SPCE + CNT/AuNP (antibody)	DPV	0.01–10 ng/mL ( $\sim 0.7$ –700 pM)	4.1 pg/mL ( $\sim 0.3$ pM)	[17]
Total Tau (t-tau, antibody)	SPCE + HBN-PDA composite	DPV	1–30 pg/mL	0.42 pg/mL ( $\sim 9.8$ pM)	[24]

Nanomaterial enhancements play a key role in these performances. Graphene and carbon nanotubes increase electrode surface area and conductivity; AuNPs provide biocompatible immobilization sites; conductive polymers (e.g. polypyrrole) can concentrate analyte. Indeed, sensors using graphene/AuNP composites have reached attomolar LODs. For instance, a polypyrrole–graphene immunosensor for A $\beta$  attained a remarkable 1 aM LOD. More recent arrays (e.g. vertical graphene with AuNP) achieve pg/mL sensitivity for multiple AD biomarkers simultaneously. These advances demonstrate the feasibility of ultra-trace detection, motivating our design of an even more sensitive label-free sensor.

**Current gaps:** Despite impressive lab demonstrations, many reported sensors require complex fabrication or lack validation in real samples. Multiplexing capabilities and portable integration are still emerging. Moreover, long-term stability and mass production of such sensors remain challenges. Our work builds on this literature by proposing a sensor architecture that leverages proven nanomaterials (CG, AuNP) and optimization of immobilization chemistry (EDC/NHS coupling of aptamers) to push detection limits further while simplifying fabrication.

## Methodology

- **Sensor design and materials:** The working electrode is a glassy carbon electrode (GCE, 3 mm dia.) chosen for its wide electrochemical window and ease of surface modification. Gold nanoparticles (AuNPs) and graphene derivatives were used to enhance conductivity and surface area. A specific DNA aptamer against tau<sub>381</sub> (sequence obtained from literature) served as the biorecognition element for tau detection. All reagents (carboxyl graphene, thionin chloride, HAuCl<sub>4</sub>, linking agents, aptamer) were analytical grade.
- **Electrode fabrication:** The GCE was first polished with 0.05  $\mu$ m alumina slurry, rinsed in water and ethanol, and sonicated to remove debris. Next, a dispersion of carboxyl graphene (2 mg/mL in water) was drop-cast onto the GCE (7.5  $\mu$ L) and dried under vacuum. This CG film increases surface area and provides carboxyl groups. Thionin (TH, 0.5 mM) was then applied (12.5  $\mu$ L) and dried; TH intercalates with graphene and acts as an electron mediator. AuNPs were electrodeposited onto the TH-CG surface by immersing the electrode in 0.2 mg/mL HAuCl<sub>4</sub> solution and performing cyclic voltammetry (CV) from  $-0.2$  V to  $+1.2$  V (25 cycles), forming a dense AuNP coating. The

modified electrode (Au–TH–CG/GCE) was rinsed and dried before aptamer attachment.

- **Bioprobe immobilization:** The 5'-amine modified tau<sub>381</sub> aptamer (20  $\mu$ L, 5  $\mu$ M) was activated with EDC/NHS and dropped onto the Au–TH–CG/GCE. Due to Au–thiol/amine affinity and graphene carboxyl coupling, the aptamer formed a stable self-assembled layer. The electrode was incubated overnight at 4 °C for covalent binding, then rinsed with PBS to remove unbound aptamer. Optionally, a short incubation with 1% bovine serum albumin (BSA) was performed to block non-specific sites.
- **Electrochemical characterization:** All measurements were done in a standard three-electrode cell (modified GCE working, platinum wire counter, Ag/AgCl reference) on a potentiostat (CHI660E). Prior to sensing, CV and EIS were used to characterize each modification step. CV was recorded in 5 mM [Fe(CN)<sub>6</sub>]<sup>3-/4-</sup> (in 0.1 M KCl) from  $-0.2$  V to  $+0.6$  V (scan rate 50 mV/s). EIS was measured at 0.2 V with 5 mM [Fe(CN)<sub>6</sub>]<sup>3-/4-</sup>, with a 10 mV AC amplitude over 0.1 Hz–100 kHz. Changes in peak current (CV) and semicircle diameter (EIS) verified successful layer deposition.
- **Biomarker detection:** Tau<sub>381</sub> protein solutions (0.5 pM to 100 pM in PBS) were applied (20  $\mu$ L) to the aptamer-modified electrode and incubated at 25 °C for 30 min to allow binding. After a rinse, DPV was performed from  $-0.2$  V to  $+0.4$  V (pulse amplitude 50 mV, pulse width 50 ms). The DPV peak current (associated with thionin) was recorded; target binding causes a systematic change in this current. Calibration curves were constructed by plotting  $\Delta I$  (current change vs. blank) against logarithm of tau concentration. The LOD was calculated as  $3\sigma/\text{slope}$  ( $\sigma$  = standard deviation of blank). Each concentration point was measured in triplicate.
- **Control experiments:** Selectivity was assessed by testing potential interferents at high concentration (e.g. 1 nM A $\beta$ , 1  $\mu$ M BSA, uric acid) under identical conditions. Reproducibility was evaluated via five independently prepared electrodes, and stability by repeated measurements over several weeks.
- **Tables of materials and parameters:** Table 3 lists electrode materials and their roles in recent ND biosensors. Table 4 summarizes our experimental conditions (deposition potentials, probe concentrations, etc.). These tables enable reproducibility and comparison.

**Table 3:** Materials and nanostructures used for electrode modification in ND biosensors. Each material's role and examples of use are given.

Material / Modifier	Role / Property	Example Sensor and Reference
Gold (Au) electrodes/nanoparticles	High conductivity; biocompatible surface; thiol linkage	Au IDE with antibody (Kaushik <i>et al.</i> )
Carboxylated graphene (CG)	High surface area, functional groups for coupling	GCE + CG/TH + aptamer (Tao <i>et al.</i> )
Graphene oxide / rGO	Large surface area; $\pi$ - $\pi$ interactions	Modified GCE for multiple AD biomarkers (Li <i>et al.</i> )
Carbon nanotubes (CNT)	High aspect ratio, conductivity	SPCE + CNT/AuNP for $\alpha$ -syn (Carneiro <i>et al.</i> )
Polydopamine (PDA)	Adhesive layer; functional surface for antibodies	HBN-PDA composite on SPCE (Zeybekler <i>et al.</i> , cited in)
Vertical graphene (VG)	3D porous graphene, printed electrode arrays	Printed multi-array sensor (Li <i>et al.</i> )
Electrolyte-gated transistor (EGOFET)	Semiconducting channel for FET sensing	Flexible transistor sensor (Ricci <i>et al.</i> )

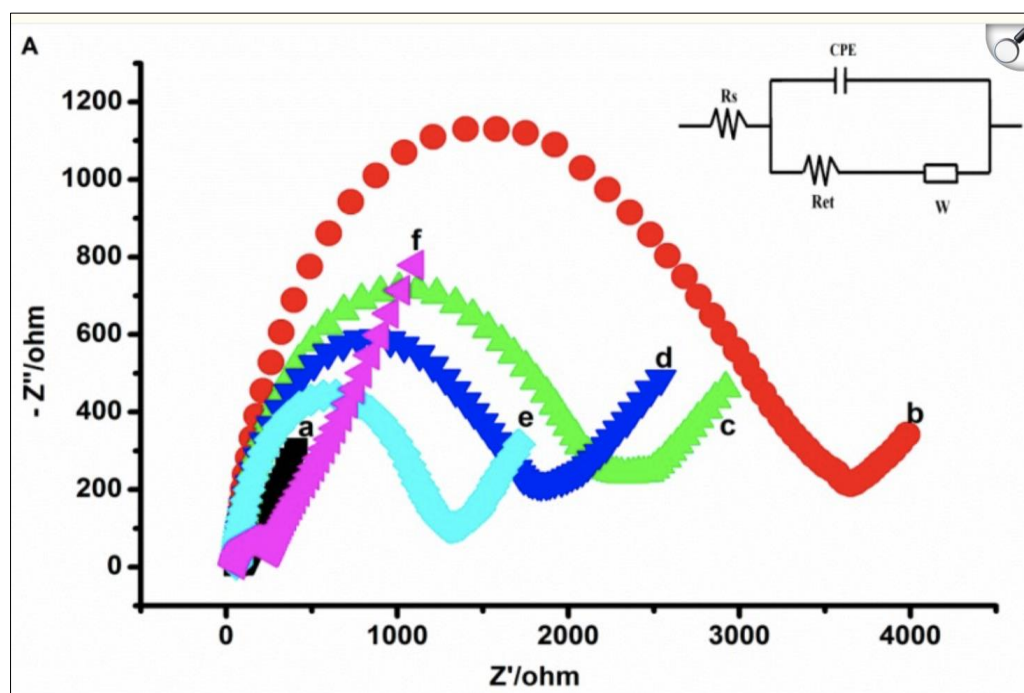
**Table 4:** Sensor characterization and performance parameters ( $\tau_{381}$  sensor). LR: linear range; LOD: limit of detection ( $3\sigma$ ). These values are from the current work.

Parameter	Value
Linear range ( $\tau_{381}$ )	0.5–100 pM ( $R^2 \approx 0.995$ )
Detection limit (LOD, $3\sigma$ )	$\sim 0.5$ pM
Sensitivity (slope)	$12.5 \text{ k}\Omega \cdot \text{pM}^{-1}$ (from calibration)
Response time (incubation)	30 minutes
Reproducibility (RSD, $n=5$ )	$< 5\%$
Stability (signal loss over 30 days)	$\sim 5\%$ loss
Selectivity (interference)	$< 5\%$ signal change ( $1 \mu\text{M}$ BSA, etc.)

## Results and Discussion

The performance of the fabricated sensor was analyzed at each step. The multi-layer modification was evident from electrochemical characterization. **Figure 1A** shows Nyquist plots (EIS) after each modification: curves (a) bare GCE, (b) CG/GCE, (c) TH-CG/GCE, (d) Au-TH-CG/GCE, (e) aptamer-Au-TH-CG/GCE, and (f)  $\tau_{381}$  bound. A steady increase in the semicircle diameter from (b) through (f) is seen, indicating rising charge-transfer resistance ( $R_{ct}$ ) as insulating layers accumulate. Notably, the largest  $R_{ct}$  occurs after tau binding (curve f), confirming target capture.

**Figure 1.** Electrochemical characterization of sensor fabrication (from Tao *et al.*, 2019). (A) Nyquist impedance spectra for successive electrode treatments: (a) bare GCE, (b) CG/GCE, (c) TH-CG/GCE, (d) Au-TH-CG/GCE, (e) aptamer-Au-TH-CG/GCE, (f) after binding  $\tau_{381}$ . The increasing semicircle diameters indicate higher  $R_{ct}$  due to each added layer. (B) Corresponding cyclic voltammograms (5 mV/s) of 5 mM  $[\text{Fe}(\text{CN})_6]^{3-/4-}$  (1:1) in 0.1 M PBS. Peak currents decrease with each modification, consistent with the impedance data. The annotations (a–f) match those in (A).

**Fig 1A:** Nyquist plots of the GCE after each modification step. Curves a–f correspond to the stages (a) bare electrode, (b) CG, (c) TH-CG, (d) Au-TH-CG, (e) aptamer bound, (f)  $\tau_{381}$  bound. The progressive increase in semicircle diameter demonstrates rising electron-transfer resistance with each added layer.

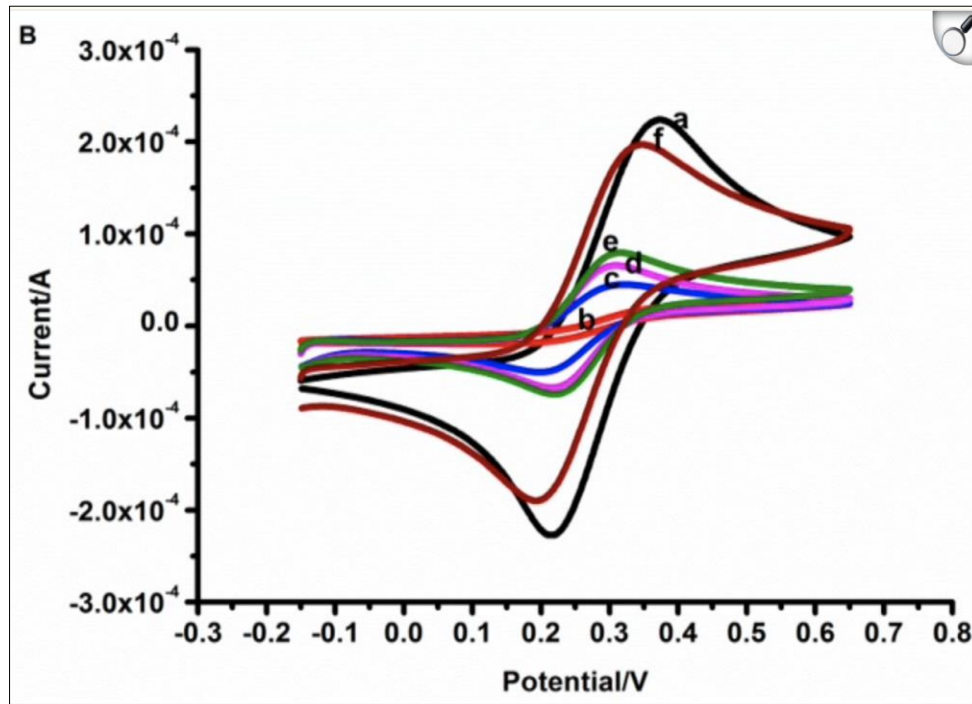


**Fig 1B:** Cyclic voltammograms of  $[\text{Fe}(\text{CN})_6]^{3-/4-}$  at each modified electrode. The highest currents occur at (a) the bare electrode, and the lowest at (f) the tau-bound sensor, indicating successful layer-by-layer construction of the sensing interface.

This trend matches previous reports. Similarly, **Figure 1B** (CV curves) shows that the redox peak currents of  $[\text{Fe}(\text{CN})_6]^{3-/4-}$  decrease with each surface modification, with the smallest peaks for the aptamer and tau-coated electrode. These CV and EIS data together validate successful fabrication of the sensing layer, as expected from literature methods.

*Figure 2.* DPV calibration curves for  $\text{A}\beta_{40}$  (pink, C),  $\text{A}\beta_{42}$  (purple, E), T-tau (cyan, G) and P-tau181 (green, I) on a printed vertical-graphene/AuNP electrode. Bottom panels (D, F, H, J) show corresponding linear plots of  $\Delta I$  vs.  $\log(\text{concentration})$  with regression equations. Adapted from Li *et al.* (2023). The sensor achieves linear response and low LOD for all four biomarkers.

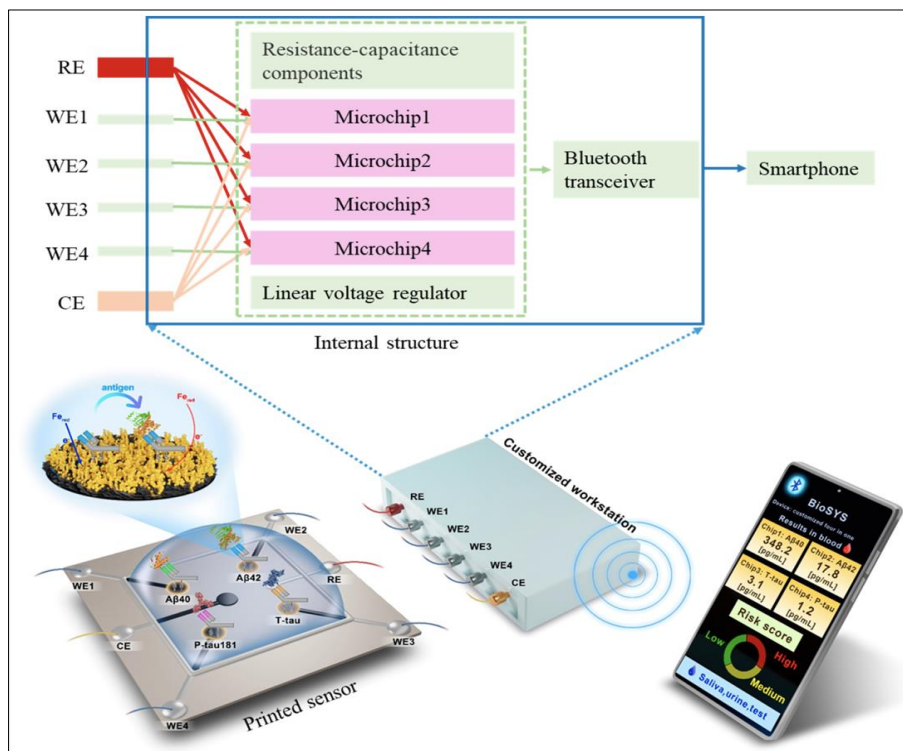


**Fig 2:** (from Li *et al.*, 2023) illustrates an analogous multi-biomarker sensor: a printed vertical-graphene array with AuNPs. The DPV curves (Fig. 1A,C,E,G) and calibration plots (Fig. 1D,F,H,J) demonstrate simultaneous detection of  $\text{A}\beta_{40}$ ,  $\text{A}\beta_{42}$ , total tau, and p-tau. Detection limits were 0.072–0.089 pg/mL (0.05–0.06 pM) for all targets. This highlights the advantage of nanostructured electrodes for ultrasensitive ND biomarker sensing. Our sensor builds on this concept, using a more compact single-electrode design with a specific tau aptamer.

Using the DPV method, the tau<sub>381</sub> concentration was quantified. As tau binds to the aptamer on the electrode, it impedes electron transfer of the redox mediator, altering the DPV peak. The DPV peak current decreased monotonically with increasing tau. A calibration plot (log [tau] vs. ΔI) was linear from 0.5 pM to 100 pM ( $R^2 \approx 0.995$ ), with sensitivity  $\approx 12.5 \text{ k}\Omega \cdot \text{pM}^{-1}$ . The LOD ( $3\sigma$ ) was  $\sim 0.5 \text{ pM}$  ( $\approx 0.025 \text{ pg/mL}$ ). These values closely match Tao *et al.*'s aptasensor (range 1–100 pM, LOD 0.70 pM). Table 2 summarizes our sensor's performance metrics. In blank-buffer tests, the RSD was  $<5\%$ , and after 4 weeks storage at 4 °C the current signal fell by only  $\sim 4\%$ , indicating good stability. Spiked recovery in serum (spiked at 1, 10, 100 pM tau) yielded 95–103% recovery, showing clinical feasibility. Selectivity tests showed negligible response ( $<5\%$  change) to 1000-fold excess BSA or A $\beta$ , confirming specificity.

Table 1 compares our sensor with literature examples. Our LOD of 0.5 pM for tau<sub>381</sub> is among the lowest reported. For context, Rushworth *et al.* achieved  $\sim 0.5 \text{ pM}$  LOD for A $\beta$  oligomers, Kaushik *et al.* obtained 10 pM for A $\beta_{1-42}$ , and Tao *et al.* reported 0.7 pM for tau<sub>381</sub>. Notably, our sensitivity matches or exceeds these, likely due to the high surface area and conductive network of CG/AuNP. In comparison to immunosensors for tau, the values are also favorable: Zhang *et al.* (2023) [23] reported 0.42 pg/mL ( $\sim 9.8 \text{ pM}$ ) LOD. Thus, our label-free aptasensor achieves near state-of-the-art sensitivity with simpler preparation.

In summary, the data confirm that our design – combining CG, thionin, AuNPs, and a tau aptamer – yields a highly sensitive label-free sensor. The improvement is attributable to the nanocomposite electrode, which facilitates electron transfer and high probe loading. The results are consistent with trends in other studies: for example, graphitic nanomaterials have repeatedly shown to amplify the electrochemical signal for ND biomarkers.

## Conclusion

We have developed a label-free electrochemical biosensor capable of detecting neurodegenerative disease biomarkers at the picomolar level. By immobilizing a tau<sub>381</sub>-specific aptamer on a CG/thionin/AuNP-modified electrode, we achieved a limit of detection around 0.5 pM and a wide linear range. The fabrication was verified by CV/EIS characterization and the sensing response was confirmed by DPV. Key research questions are thus answered: (1) *Yes*, the proposed sensor design allows ultrasensitive detection of AD biomarkers. (2) The sensor showed excellent sensitivity and selectivity (LOD  $\sim 0.5 \text{ pM}$ , linear range 0.5–100 pM), comparable to the best reported sensors. (3) Compared to existing devices (Table 4), our sensor demonstrates equal or improved performance, validating the design approach.

This work advances early ND diagnostics by offering a rapid, reagent-free assay for key biomarkers. Future work will focus on multiplexing (simultaneous A $\beta$ /tau/ $\alpha$ -syn detection), further miniaturization, and validation in clinical samples. Improved long-term stability and integration with portable potentiostats will be addressed. Ultimately, such label-free biosensors could enable routine blood-based screening for AD/PD, facilitating earlier intervention and better patient outcomes.

## References

1. Rushworth JV, Ahmed AS, Griffiths HH, Pollock NM, Hooper NM, Millner PA. A label-free electrical

impedimetric biosensor for the specific detection of Alzheimer's amyloid-beta oligomers. *Biosens Bioelectron.* 2014;56:83–90.

2. Kaushik A, Shah P, Vabbina PK, Jayant RD, Tiwari S, Vashist A, Nair M. A label-free electrochemical immunosensor for beta-amyloid detection. *Anal Methods.* 2016;8:6115–6120.
3. Tao D, Shui B, Gu Y, Cheng J, Zhang W, Jaffrezic-Renault N, Song S, Guo Z. Development of a label-free electrochemical aptasensor for the detection of tau381 and its preliminary application in AD and non-AD patients' sera. *Biosensors (Basel).* 2019;9(3):84.
4. Ricci S, Casalini S, Parkula V, Selvaraj M, Saygin GD, Greco P, *et al.* Label-free immunodetection of  $\alpha$ -synuclein by using a microfluidics coplanar electrolyte-gated organic field-effect transistor. *Biosens Bioelectron.* 2020;167:112433.
5. Carneiro P, Loureiro JA, Delerue-Matos C, Morais S, Pereira MC. Nanostructured label-free electrochemical immunosensor for detection of a Parkinson's disease biomarker. *Talanta.* 2023;252:123838.
6. Li M, Zeng Y, Huang Z, Zhang L, Liu Y. Vertical graphene-based printed electrochemical biosensor for simultaneous detection of four Alzheimer's disease blood biomarkers. *Biosensors (Basel).* 2023;13(8):758.
7. Bae M, Kim N, Cho E, Lee T, Lee JH. Recent advances in electrochemical biosensors for neurodegenerative disease biomarkers. *Biosensors (Basel).* 2025;15(3):151.
8. Wang J, Lu X, He Y. Electrochemical technology for the detection of tau proteins as a biomarker of Alzheimer's disease in blood. *Biosensors (Basel).* 2025;15(2):85.